2016 IEEE 55th Conference on Decision and Control (CDC)
ARIA Resort & Casino
December 12-14, 2016, Las Vegas, USA

Robustness of Adaptive Control for Three-Dimensional Curve Tracking under State Constraints: Effects of Scaling Control Terms

Michael Malisoff Robert Sizemore Fumin Zhang

Abstract— **In a recent *SIAM Journal on Control and Optimization* article, our team analyzed the robustness of a class of adaptive three-dimensional curve tracking controls for free moving particles, using penalty functions and robustly forward invariant sets with maximum allowable perturbation bounds. This allowed us to track curves, identify unknown control gains, and provide predictable tolerance and safety bounds. In this work, we provide a variant of our SIAM article. We provide a new method to maintain robust forward invariance of compact regions in the state space, under arbitrarily large perturbation bounds. Our new technique entails scaling certain control components. It provides a substantially different algorithm from our SIAM article and is suitable for real time applications.**

Key Words: **Curve tracking, robotics, robustness.**

I. Introduction

This paper continues our search for ways to ensure curve tracking under the uncertainties and state constraints that prevail in robotics. See [9], [11], and our earlier conference papers for two-dimensional (2D) curve tracking; and [12] [13], and [14] for three-dimensional (3D) analogs. Our search was motivated by our group's 2011 field work at Grand Isle, LA, which used marine robots and curve tracking controls to study residual pollution from the 2010 Deepwater Horizon oil spill disaster in the Gulf of Mexico; see [16], and see [6], [18], [19], and [23] for more motivation.

Curve tracking aims to ensure that robots converge to a parallel tracking of a desired curve, and has been studied for over 20 years; see [1], [2], [17], and [20]. Asymptotic tracking under curve tracking controllers was shown using nonstrict Lyapunov functions and other traditional methods; see [2], [17], and [20]. Through experiments, the controls were shown to give good performance, even under severe perturbations, in farming [7], obstacle avoidance in corridors [21], and ocean sampling [20]. However, experiments do not ensure robustness to perturbations under all possible conditions, because only finitely many operating conditions can be tested in finite time, and experiments can be costly and hazardous. Hence, experiments do not lend themselves to the search for values for the maximum allowable perturbations.

This motivated our more mathematical approaches. One general strategy to ensure robustness is 'strictification', which converts nonstrict Lyapunov functions into strict ones; see [8] and [15]. By strictness, we mean that its time derivative is negative along all trajectories of the closed loop system at all points outside the equilibrium. Strict Lyapunov functions are useful for proving input-to-state stability (ISS) under uncertainty [3], and for redesigning controllers to achieve ISS with respect to perturbations. See, e.g., [9] where we converted a nonstrict Lyapunov function from [21] for 2D curve tracking into a strict one, and [14] for 3D analogs.

Although strict Lyapunov functions are effective for backstepping, ISS, and much more, they may not be sufficient for state constrained problems where one seeks tolerance and safety bounds. This is because Lyapunov decay estimates may give conservative estimates for the largest possible perturbations for maintaining forward invariance of sublevel sets of Lyapunov functions [14]. Therefore, our work [9] combined strict Lyapunov functions with robust forward invariance for 2D hexagons, including formulas for largest allowable perturbations for ensuring forward invariance of the hexagons. Then [13] and [14] generalized the approach from [9] to 3D, using paired hexagons. Robust forward invariance of a set $\mathscr{H}$ for a system $\dot{X}(t) = \mathscr{F}(t, X(t), \delta(t))$ means forward invariance of $\mathscr{H}$ for all measurable bounded perturbations $\delta : [0, \infty) \to \mathscr{D}$, or equivalently, strong forward invariance of $\mathscr{H}$ for the inclusion $\dot{X}(t) \in \mathscr{F}(t, X(t), \mathscr{D})$, where $\mathscr{D}$ is the set of all allowable values for δ [14]. Hence, robust forward invariance means that all solutions starting in $\mathscr{H}$ stay in $\mathscr{H}$, regardless of which $\mathscr{D}$ valued measurable essentially bounded function is used in the system.

A key observation from [14, Remark 2] is that for fixed penalty functions in the control and a fixed desired bounding set $\mathscr{D}$ for the perturbations, we can build the hexagon pairs (depending on $\mathscr{D}$ and the control) to ensure robust forward invariance of the hexagon pairs under all $\mathscr{D}$ valued perturbations. However, a potential drawback was that larger $\mathscr{D}$'s led to robustly forwardly invariant hexagon pairs that include points that are very close to the boundary of the workspace, as well as points that correspond to the robot being very far from the curve being tracked, and an analogous statement holds for 2D curve tracking. Since this can allow robots to move close to undesirable regions, it can be a disadvantage.

To help overcome the preceding challenge in the 2D case, our work [10] used the following scaling algorithm to compensate for arbitrarily large perturbation bounds. First, we fixed any suitable 2D hexagon shaped compact region $\mathscr{H}$ in the workspace and a value $\bar{\delta} > 0$ for the perturbation bound. Then, we scaled the steering constant and the penalty functions in the control by a constant $\mathscr{M}_* \geq 1$ (depending on $\mathscr{H}$ and $\bar{\delta}$) and proved robust forward invariance of $\mathscr{H}$ for

Malisoff and Sizemore are with the Department of Mathematics, Louisiana State University, 303 Lockett Hall, Baton Rouge, LA 70803-4918, malisoff@lsu.edu and rsizem2@lsu.edu. Zhang is with the School of Electrical and Computer Engineering, Georgia Institute of Technology, 85 Fifth Street NW, Atlanta, GA 30332-0250, fumin@gatech.edu. Malisoff was supported by NSF Grant ECCS-1408295. Zhang was supported by ONR Grants N00014-08-1-1007 and N00014-09-1-1074, and NSF Grants ECCS-0841195, ECCS-0845333 (CAREER), ECCS-1056253, and CNS-0931576.

the closed loop system under all scalar perturbations that are bounded by $\bar{\delta}$. This eliminated the need to move the hexagon legs too close or far from the boundary of the workspace, and can help ensure robust, safe operation under perturbations.

In this note, we extend the 2D scaling approach from [10] to the 3D curve tracking dynamics from [14], to ensure tracking under control uncertainty and state constraints and identification of unknown control gains under arbitrarily large perturbation bounds using adaptive control; see [4] and [5] for background on adaptive control. As in [10], a benefit of the new method in this note is that it eliminates the need to include points in the hexagons that may be too close to the boundary of the state space. However, while [10] used only one scaling constant, our 3D dynamics will lead us to use three different scaling constants. We can extend this approach to cover input delays, by converting our strict Lyapunov functions into Lyapunov-Krasovskii functionals, using ideas from [14, Section 7.4]. Due to length restrictions, we will not include time delays here, but the effects of input delays can be captured by the perturbation terms using a variant of [14, Section 6.3] that we leave to the reader.

II. Background and Main Results from [14]

To make our work more self contained, we review the 3D curve tracking model and robust forward invariant sets from [14]. Then we present our new work, starting in Section III.

A. Model and Controls

The model describes the motion of a free particle, and a second particle (called the closest or projection point) that is confined to a specified 3D curve and that locally has the shortest distance to the free particle. Let $\mathbf{r_1}$ be the position of the second particle, $\mathbf{x_1}$ be the unit tangent vector to the curve at $\mathbf{r_1}$, $\mathbf{y_1}$ be a unit normal vector, and $\mathbf{z_1}$ be a binormal. The velocity of the point is in the direction of $\mathbf{x_1}$.

Let $\mathbf{r_2}$ be the position of the free particle moving at unit speed, $\mathbf{x_2}$ be the unit tangent vector to the trajectory of its moving center, $\mathbf{y_2}$ be a corresponding unit normal vector, and $\mathbf{z_2} = \mathbf{x_2} \times \mathbf{y_2}$. With the speed $\frac{ds}{dt} = \alpha$, the dynamics of the free point and the closest point on the curve from [14] and [22] are

$$\begin{array}{rclrcl} \dot{\mathbf{r}}_1 &=& \alpha \mathbf{x_1} & \dot{\mathbf{r}}_2 &=& \mathbf{x_2} \\ \dot{\mathbf{x}}_1 &=& \alpha\kappa_n \mathbf{y_1} + \alpha\kappa_g \mathbf{z_1} & \dot{\mathbf{x}}_2 &=& u\mathbf{y_2} + v\mathbf{z_2} \\ \dot{\mathbf{y}}_1 &=& -\alpha\kappa_n \mathbf{x_1} & \dot{\mathbf{y}}_2 &=& -u\mathbf{x_2} \\ \dot{\mathbf{z}}_1 &=& -\alpha\kappa_g \mathbf{x_1}, & \dot{\mathbf{z}}_2 &=& -v\mathbf{x_2}, \end{array} \tag{1}$$

where the normal curvature κ_n and the geodesic curvature κ_g are associated with the curve at the closest point, and the steering controls u and v we will chosen later.

Following [14], we write the controls as

$$\begin{array}{l} u = a_1(\mathbf{x_1}\cdot\mathbf{y_2}) + a_2(\mathbf{y_1}\cdot\mathbf{y_2}) + a_3(\mathbf{z_1}\cdot\mathbf{y_2}) \text{ and} \\ v = a_1(\mathbf{x_1}\cdot\mathbf{z_2}) + a_2(\mathbf{y_1}\cdot\mathbf{z_2}) + a_3(\mathbf{z_1}\cdot\mathbf{z_2}), \end{array} \tag{2}$$

where the coefficients a_i will be specified. We also set $\rho_1 = (\mathbf{r_2} - \mathbf{r_1})\cdot\mathbf{y_1}$ and $\rho_2 = (\mathbf{r_2} - \mathbf{r_1})\cdot\mathbf{z_1}$, and we use the shape variables $\varphi = \mathbf{x_1}\cdot\mathbf{x_2}$, $\beta = \mathbf{y_1}\cdot\mathbf{x_2}$, and $\gamma = \mathbf{z_1}\cdot\mathbf{x_2}$, and the spherical coordinate transformation $(\varphi,\beta,\gamma) = \big(\cos(\zeta)\cos(\theta), -\sin(\zeta)\cos(\theta), \sin(\theta)\big)$. Finally, we choose

$$a_1 = \mu,\ a_2 = -h_1'(\rho_1) + \tfrac{\alpha\kappa_n}{\varphi} \text{ and } a_3 = -h_2'(\rho_2) + \tfrac{\alpha\kappa_g}{\varphi}, \tag{3}$$

where $\mu > 0$ is any fixed constant called the steering constant and the C^1 penalty functions $h_i : (0,\infty) \to [0,\infty)$ are

$$h_i(\rho_i) = \begin{cases} \bar{h}_i\left(\rho_i + \frac{\rho_{ci}^2}{\rho_i} - 2\rho_{ci}\right), & \rho_i \in (0,\rho_{ci}) \\ \frac{\bar{h}_i}{\rho_{ci}}(\rho_i - \rho_{ci})^2, & \rho_i \geq \rho_{ci} \end{cases} \tag{4}$$

for $i = 1,2$ for fixed constants $\bar{h}_i > 0$ and $(\rho_{c1},\rho_{c2}) \in (0,\infty)^2$, and we assume that κ_n and κ_g are C^1, bounded, and non-positive valued. Then $\alpha = \varphi/(1 - \kappa_n\rho_1 - \kappa_g\rho_2)$ [14]. This is a slight generalization of the controls from [14], which required that $\bar{h}_1 = \bar{h}_2$. Our basic tracking goal is to ensure that $\lim_{t\to\infty}(\rho_1,\zeta,\rho_2,\theta)(t) = (\rho_{c1},0,\rho_{c2},0)$ for all initial conditions, to ensure parallel motion relative to the curve that is being tracked while maintaining sufficient separation between the robot and the curve [14]. Our state constraints will ensure that the ρ_i's and φ stays positive.

Using [14, Section 5.2] (except with different $\bar{h}_i$ used in the penalty functions h_i) with the control components (3) scaled by $G/\hat{G}$, we obtain the augmented adaptive 3D curve tracking dynamics with parameter estimate $\hat{G}$ given by

$$\begin{array}{rcl} \dot{\rho}_1 &=& -\sin(\zeta)\cos(\theta) \\ \dot{\zeta} &=& -\frac{\cos(\zeta)\kappa_n}{1-\kappa_n\rho_1-\kappa_g\rho_2}\frac{1}{\cos(\theta)}\left(\frac{G}{\hat{G}} - \cos^2(\theta)\right) \\ && -\frac{\alpha\kappa_g\sin(\theta)\sin(\zeta)}{\cos(\theta)} \\ && +\frac{G}{\hat{G}}\frac{h_1'(\rho_1)\cos(\zeta)}{\cos(\theta)} - \frac{G}{\hat{G}}\frac{\mu\sin(\zeta)}{\cos(\theta)} + \delta_1 \\ \dot{\rho}_2 &=& \sin(\theta) \\ \dot{\theta} &=& -\frac{\kappa_g\cos^2(\zeta)\cos(\theta)}{1-\kappa_n\rho_1-\kappa_g\rho_2} + \frac{G}{\hat{G}}\left(-h_1'(\rho_1)\right. \\ && \left.+\frac{\kappa_n}{1-\kappa_n\rho_1-\kappa_g\rho_2}\right)\sin(\zeta)\sin(\theta) \\ && +\left[\frac{G}{\hat{G}}\left(-h_2'(\rho_2) + \frac{\kappa_g}{1-\kappa_n\rho_1-\kappa_g\rho_2}\right)\cos(\theta)\right] \\ && -\frac{G}{\hat{G}}\mu\cos(\zeta)\sin(\theta) + \delta_2 \\ \dot{\hat{G}} &=& \frac{(g_{\max}-\hat{G})(\hat{G}-g_{\min})}{\hat{G}}\left(\frac{\partial U}{\partial\zeta}\mathscr{A}_1(Y) + \frac{\partial U}{\partial\theta}\mathscr{A}_2(Y)\right) \end{array} \tag{5}$$

on the augmented state space $\mathscr{X}_a = (0,\infty)\times(-\pi/2,\pi/2)\times(0,\infty)\times(-\pi/2,\pi/2)\times(g_{\min},g_{\max})$, where the unknown measurable essentially bounded functions δ_i represent uncertainty, G is an unknown control gain (i.e., an unknown positive constant that multiplies the control components in the system) that is known to lie on some interval $(g_{\min},g_{\max})$ with known positive endpoints $g_{\min}$ and $g_{\max}$, the functions $\mathscr{A}_i(Y)$ of the state $Y = (\rho_1,\zeta,\rho_2,\theta)$ are

$$\begin{array}{rcl} \mathscr{A}_1(Y) &=& -\frac{1}{\cos(\theta)}\left[\left(\frac{\kappa_n}{1-\kappa_n\rho_1-\kappa_g\rho_2} - h_1'(\rho_1)\right)\cos(\zeta)\right. \\ && \left.+\mu\sin(\zeta)\right], \text{ and} \\ \mathscr{A}_2(Y) &=& -\mu\cos(\zeta)\sin(\theta) \\ && +\left(\frac{\kappa_n}{1-\kappa_n\rho_1-\kappa_g\rho_2} - h_1'(\rho_1)\right)\sin(\zeta)\sin(\theta) \\ && +\left(\frac{\kappa_g}{1-\kappa_n\rho_1-\kappa_g\rho_2} - h_2'(\rho_2)\right)\cos(\theta), \end{array} \tag{6}$$

where Y is valued in $\mathscr{X} = (0,\infty)\times(-\pi/2,\pi/2)\times(0,\infty)\times(-\pi/2,\pi/2)$, and

$$\begin{array}{l} U(\rho_1,\zeta,\rho_2,\theta) = -h_1'(\rho_1)\sin(\zeta)\cos(\theta) \\ +h_2'(\rho_2)\sin(\theta) + \int_0^{V(\rho_1,\zeta,\rho_2,\theta)}\mathscr{L}_0(q)\mathrm{d}q, \text{ where} \end{array} \tag{7}$$

$$\begin{array}{l} V(\rho_1,\zeta,\rho_2,\theta) = \\ -\ln(\cos(\theta)) - \ln(\cos(\zeta)) + h_1(\rho_1) + h_2(\rho_2) \end{array} \tag{8}$$

and

$$\begin{aligned}\mathscr{L}_0(q) &= \tfrac{3}{\mu}\left[\Gamma(q)+1\right]\left(1+||\kappa_n||_\infty+||\kappa_g||_\infty\right)\\ &\quad +2\left[\tfrac{1}{\mu}\lambda(q)+\Gamma'(q)+1\right],\end{aligned} \tag{9}$$

and $\lambda(q)=\lambda_0(q,\rho_{c1})+\lambda_0(q,\rho_{c2})+2\bar{c}/\min\{\rho_{c1},\rho_{c2}\}$ and $\Gamma(q)=\Gamma_0(q,\rho_{c1})+\Gamma_0(q,\rho_{c2})+4\bar{c}q/\min\{\rho_{c1},\rho_{c2}\}$, with the choices $\bar{c}=\max\{\bar{h}_1,\bar{h}_2\}$ and

$$\begin{aligned}&\lambda_0(q,\rho_{ci})=\tfrac{2}{\bar{c}^2\rho_{ci}^4}(q+2\bar{c}\rho_{ci})^3+1+0.5(\mu)^2+\mu\\ &\text{and }\ \Gamma_0(q,\rho_{ci})=\tfrac{18\bar{c}}{\rho_{ci}}q+\left(\tfrac{2}{\rho_{ci}}\right)^4\tfrac{9q^4}{\bar{c}^2}\ .\end{aligned} \tag{10}$$

Here and in what follows, $||\cdot||_\infty$ (resp., $||\cdot||_{\mathscr{I}}$) denotes the sup norm (resp., sup over any set $\mathscr{I}$).

When the parameter estimate $\hat{G}$ for the unknown parameter G is equal to G, our system (5) can be written as [14]

$$\begin{aligned}\dot{\rho}_1 &= -\sin(\zeta)\cos(\theta)\\ \dot{\zeta} &= \delta_1-\tfrac{1}{\cos^2(\theta)}\left[\alpha\kappa_n\sin^2(\theta)\right.\\ &\quad +\alpha\kappa_g\sin(\theta)\sin(\zeta)\cos(\theta)\\ &\quad \left.-h_1'(\rho_1)\cos(\zeta)\cos(\theta)+\mu\sin(\zeta)\cos(\theta)\right]\\ \dot{\rho}_2 &= \sin(\theta)\\ \dot{\theta} &= \alpha\kappa_g\tfrac{\sin^2(\zeta)}{\cos(\zeta)}-h_2'(\rho_2)\cos(\theta)\\ &\quad +\left(-h_1'(\rho_1)+\tfrac{\alpha\kappa_n}{\cos(\theta)\cos(\zeta)}\right)\sin(\zeta)\sin(\theta)\\ &\quad -\mu\cos(\zeta)\sin(\theta)+\delta_2\end{aligned} \tag{11}$$

on the state space $\mathscr{X}=(0,\infty)\times(-\pi/2,\pi/2)\times(0,\infty)\times(-\pi/2,\pi/2)$, which we call the nonadaptive dynamics, and in the special case where the perturbations δ_i are identically zero in (11), we call (11) the unperturbed nonadaptive dynamics. The motivation for (7) is that U is a strict Lyapunov function for the unperturbed nonadaptive dynamics on $\mathscr{X}$ with respect to its equilibrium $\mathscr{E}=(\rho_{c1},0,\rho_{c2},0)$; see [14, Theorem 2]. The barrier term $(g_{\max}-\hat{G})(\hat{G}-g_{\min})$ in (5) ensures that the parameter estimate $\hat{G}$ stays in the interval $(g_{\min},g_{\max})$ that contains G. We can use a variant of the proof of [14, Theorem 5] (with a scaling of the h_i's by different constants $\bar{h}_i$, and with the δ_i's set equal to 0) to show this curve tracking and parameter identification result:

Theorem 1: When the δ_i's are zero, the dynamics (5) are uniformly globally asymptotically stable to the equilibrium $(\rho_{c1},0,\rho_{c2},0,G)$ on its state space $\mathscr{X}_a=(0,\infty)\times(-\pi/2,\pi/2)\times(0,\infty)\times(-\pi/2,\pi/2)\times(g_{\min},g_{\max})$. □

B. Robust Forward Invariance

The preceding subsection leaves open the problem of finding largest possible perturbation sets $\mathscr{D}\subseteq\mathbb{R}^2$ such that all solutions of the Y subsystem in (5), for all measurable essentially bounded choices of $\delta=(\delta_1,\delta_2):[0,\infty)\to\mathscr{D}$, that start in suitable subsets $\mathscr{H}$ of $\mathscr{X}$ remain in $\mathscr{H}$ at all future times. In [14], we solved the preceding robust forward invariant problem by choosing the sets $\mathscr{H}\subseteq\mathscr{X}$ to be paired hexagons and the allowable perturbation sets to be compact subsets of maximal boxes $\mathscr{D}$. The $\mathscr{D}$'s were maximal in the sense that for each constant perturbation $\bar{d}$ that takes a value outside $\mathscr{D}$, there existed a point p_* on the boundary of $\mathscr{H}$ such that the corresponding solution of the nonadaptive dynamics (11) starting at p_* for the perturbation $\bar{d}$ exits $\mathscr{H}$ in finite time. The analysis in [14] assumes that $\bar{h}_1=\bar{h}_2$, but it carries over to the case where these constants can differ.

Given any quadruple $(\rho_{*1},\rho_{*2},K_1,K_2)\in(0,\rho_{c1})\times(0,\rho_{c2})\times[\rho_{c1},\infty)\times[\rho_{c2},\infty)$ and any constants $\bar{\zeta}\in(0,\pi/2)$ and $\bar{\theta}\in(0,\pi/2)$, the robustly forwardly invariant sets in [14] took the form $\mathscr{H}=H_1(\rho_{*1},\bar{\zeta},K_1)\times H_2(\rho_{*2},\bar{\theta},K_2)$, where $H_1(\rho_{*1},\bar{\zeta},K_1)$ is the closed set in the (ρ_1,ζ) plane whose boundary is the hexagon that has the vertices $A=(\rho_{*1},0)$, $B=(\rho_{*1}+\bar{\zeta}/\mu^\sharp,\bar{\zeta})$, $C=(\rho_{*1}+2\bar{\zeta}/\mu^\sharp+K_1,\bar{\zeta})$, $D=(\rho_{*1}+2\bar{\zeta}/\mu^\sharp+K_1,0)$, $E=(\rho_{*1}+\bar{\zeta}/\mu^\sharp+K_1,-\bar{\zeta})$, and $F=(\rho_{*1},-\bar{\zeta})$, and $H_2(\rho_{*2},\bar{\theta},K_2)$ is the closed set in the (ρ_2,θ) plane whose boundary is the hexagon with the vertices $A'=(\rho_{*2},0)$, $B'=(\rho_{*2},\bar{\theta})$, $C'=(\rho_{*2}+\bar{\theta}/(\mu^\sharp\cos(\bar{\zeta}))+K_2,\bar{\theta})$, $D'=(\rho_{*2}+2\bar{\theta}/(\mu^\sharp\cos(\bar{\zeta}))+K_2,0)$, $E'=(\rho_{*2}+2\bar{\theta}/(\mu^\sharp\cos(\bar{\zeta}))+K_2,-\bar{\theta})$, and $F'=(\rho_{*2}+\bar{\theta}/(\mu^\sharp\cos(\bar{\zeta})),-\bar{\theta})$, where $\mu^\sharp=\mu g_{\min}/g_{\max}$, and the corresponding perturbation sets had the form $\mathscr{D}=[-\delta_{*1},\delta_{*1}]\times[-\delta_{*2},\delta_{*2}]$ for suitable maximum constant bounds δ_{*i} for $i=1$ and 2. See Figure 1.

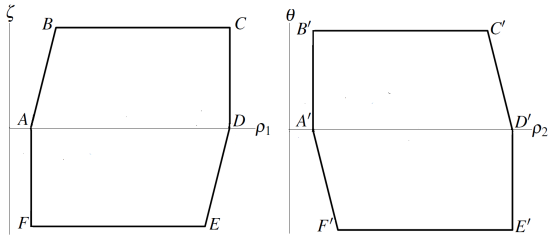

Fig. 1. Hexagon Shaped Boundaries of Sets $H_1(\rho_{*1},\bar{\zeta},K_1)$ (Left) and $H_2(\rho_{*2},\bar{\theta},K_2)$ (Right) for Robustly Forwardly Invariant Set $H_1(\rho_{*1},\bar{\zeta},K_1)\times H_2(\rho_{*2},\bar{\theta},K_2)$

Also, [14, Remark 2] showed that for each pair $(\delta_{*1},\delta_{*2})\in(0,\infty)$, we can chose the K_i's and ρ_{*i}'s and μ such that $\mathscr{H}$ is robustly forwardly invariant for the dynamics (11) with the perturbation set $\mathscr{D}$. However, as the δ_{*i}'s become large, the required ρ_{*i}'s converge to 0, and the required K_i's converge to ∞, which may be a disadvantage, since small ρ_{*i}'s correspond to allowing the robot to get very close to the curve, and large K_i's allow the robot to get very far from the curve. Our new results that we present next help overcome this disadvantage.

III. Robust Forward Invariance under Scaling

The remainder of this work is new theory that has not appeared previously and substantially differs from [14]. Since the barrier term $(g_{\max}-\hat{G})(\hat{G}-g_{\min})$ in (5) keeps the parameter estimate $\hat{G}$ in the interval $(g_{\min},g_{\max})$ [14], and since there are no perturbations in the parameter update law

$$\dot{\hat{G}}=(g_{\max}-\hat{G})(\hat{G}-g_{\min})\tfrac{1}{\hat{G}}\left(\tfrac{\partial U}{\partial\zeta}\mathscr{A}_1(Y)+\tfrac{\partial U}{\partial\theta}\mathscr{A}_2(Y)\right) \tag{12}$$

from (5), it suffices to prove robust forward invariance for the $Y=(\rho_1,\zeta,\rho_2,\theta)$ subsystem of (5) on subsets of $\mathscr{X}=(0,\infty)\times(-\pi/2,\pi/2)\times(0,\infty)\times(-\pi/2,\pi/2)$ for each choice of $\hat{G}(t)$. To this end, we first rewrite this Y subsystem as

$$\left\{\begin{aligned}\dot{\rho}_1 &= -\sin(\zeta)\cos(\theta)\\ \dot{\zeta} &= \mathscr{Q}_1(Y,\hat{G},\mu,\bar{h})+\delta_1\\ \dot{\rho}_2 &= \sin(\theta)\\ \dot{\theta} &= \mathscr{Q}_2(Y,\hat{G},\mu,\bar{h})+\delta_2,\end{aligned}\right. \tag{13}$$

where

$$\begin{aligned}\mathscr{Q}_1(Y,\hat{G},\mu,\bar{h}) &= -\tfrac{\cos(\zeta)\kappa_n}{1-\kappa_n\rho_1-\kappa_g\rho_2}\tfrac{1}{\cos(\theta)}\left(\tfrac{G}{\hat{G}}-\cos^2(\theta)\right)\\ &-\tfrac{\alpha\kappa_g\sin(\theta)\sin(\zeta)}{\cos(\theta)}+\tfrac{G}{\hat{G}}\tfrac{h_1'(\rho_1)\cos(\zeta)}{\cos(\theta)}-\tfrac{G}{\hat{G}}\tfrac{\mu\sin(\zeta)}{\cos(\theta)} \text{ and}\end{aligned} \tag{14}$$

$$\begin{aligned}\mathscr{Q}_2(Y,\hat{G},\mu,\bar{h}) &= -\tfrac{\kappa_g\cos^2(\zeta)\cos(\theta)}{1-\kappa_n\rho_1-\kappa_g\rho_2}\\ &+\tfrac{G}{\hat{G}}\left(-h_1'(\rho_1)+\tfrac{\kappa_n}{1-\kappa_n\rho_1-\kappa_g\rho_2}\right)\sin(\zeta)\sin(\theta)\\ &+\tfrac{G}{\hat{G}}\left(-h_2'(\rho_2)+\tfrac{\kappa_g}{1-\kappa_n\rho_1-\kappa_g\rho_2}\right)\cos(\theta)-\tfrac{G\mu\cos(\zeta)\sin(\theta)}{\hat{G}},\end{aligned} \tag{15}$$

where we leave out the dependencies of the $\mathscr{Q}_i$'s on t (through the time-varying curvatures κ_n and κ_g) to simplify the notation. The preceding functions agree with the $\mathscr{Q}_i^{\mathscr{A}}$'s in [14], but we write them as $\mathscr{Q}_i(Y,\hat{G},\mu,\bar{h})$'s to emphasize their dependence on the constant choices of μ and $\bar{h}=(\bar{h}_1,\bar{h}_2)$.

However, unlike in [14] where we computed the maximum allowable bounds for the perturbations to maintain forward invariance of $\mathscr{H}=H_1(\rho_{*1},\bar{\zeta},K_1)\times H_2(\rho_{*2},\bar{\theta},K_2)$, here we do the following. First, we fix a disturbance set $\bar{\mathscr{D}}=[-\bar{\Delta}_1,\bar{\Delta}_1]\times[-\bar{\Delta}_2,\bar{\Delta}_2]$ that is known to contain all $\delta(t)$ values, where the $\bar{\Delta}_i$'s are any known nonnegative constants. Then, we choose μ and the $\bar{h}_i$'s to ensure that $\mathscr{H}=H_1(\rho_{*1},\bar{\zeta},K_1)\times H_2(\rho_{*2},\bar{\theta},K_2)$ is robustly forwardly invariant for (13) with perturbations $\delta:[0,\infty)\to\bar{\mathscr{D}}$, where the constants $\rho_{*i}\in(0,\rho_{ci})$ and $K_i\in[\rho_{ci},\infty)$ for $i=1,2$, $\bar{\zeta}\in(0,\pi/2)$, and $\bar{\theta}\in(0,\pi/2)$ are fixed; see Section IV for a detailed comparison between the method in [14] and the one we provide here, including algorithms for applying both methods.

Enlarging μ increases the slopes of the tilted legs AB and DE in Fig. 1 and decreases the slopes of the legs A′F′ and C′D′, so our new hexagons have the same general shape as in Fig. 1 but become more like boxes. Also, for each constant $\bar{\mu}\geq 1$, we have

$$\begin{aligned}(\rho_{c1},0) &\in H_1(\rho_{*1},\bar{\zeta},K_1)\\ &\subseteq \left[\rho_{*1},\rho_{*1}+\tfrac{2\bar{\zeta}}{\bar{\mu}}+K_1\right]\times[-\bar{\zeta},\bar{\zeta}] \text{ and}\\ (\rho_{c2},0) &\in H_2(\rho_{*2},\bar{\theta},K_2)\\ &\subseteq \left[\rho_{*2},\rho_{*2}+\tfrac{2\bar{\theta}}{\bar{\mu}\cos(\bar{\zeta})}+K_2\right]\times[-\bar{\theta},\bar{\theta}]\end{aligned} \tag{16}$$

for all choices of $\mu^\sharp=\mu g_{\min}/g_{\max}\geq\bar{\mu}$, so the hexagons maintain a positive distance of $\min\{\rho_{*1},\rho_{*2},\pi/2-\bar{\zeta},\pi/2-\bar{\theta}\}$ from the boundary of $\mathscr{X}$ for all choices of $\mu^\sharp\geq\bar{\mu}$. On the other hand, it is impossible to prove robust forward invariance of boxes instead of hexagons; see [14, Remark 4].

Our new robust forward invariance result will follow from this analogue of [14, Lemma 4], which will lead to our new robust forward invariance algorithm in Section IV:

Theorem 2: Let $(\rho_{*1},\rho_{*2},K_1,K_2,\bar{\zeta},\bar{\theta},\bar{\Delta}_1,\bar{\Delta}_2)\in(0,\rho_{c1})\times(0,\rho_{c2})\times[\rho_{c1},\infty)\times[\rho_{c2},\infty)\times(0,\pi/2)^2\times[0,\infty)^2$ be any constant vector. Then we can choose the constants $\bar{h}_i>0$ in the penalty functions h_i in (4), and the constant $\mu\geq 1$ in (3), such that the following four conditions E1-E4 are satisfied:

- E1 $\mathscr{Q}_1(Y,\hat{G},\mu,\bar{h})+\mu^\sharp\sin(\zeta)\cos(\theta)>\bar{\Delta}_1$ for all $(\rho_1,\zeta)\in ED$ and all $(\rho_2,\theta)\in H_2(\rho_{*2},\bar{\theta},K_2)$. Also, $\mathscr{Q}_1(Y,\hat{G},\mu,\bar{h})+\mu^\sharp\sin(\zeta)\cos(\theta)<-\bar{\Delta}_1$ for all $(\rho_1,\zeta)\in AB$ and all $(\rho_2,\theta)\in H_2(\rho_{*2},\bar{\theta},K_2)$.
- E2 $\mathscr{Q}_1(Y,\hat{G},\mu,\bar{h})>\bar{\Delta}_1$ for all $(\rho_1,\zeta)\in FE$ and all $(\rho_2,\theta)\in H_2(\rho_{*2},\bar{\theta},K_2)$. Also, $\mathscr{Q}_1(Y,\hat{G},\mu,\bar{h})<-\bar{\Delta}_1$ for all $(\rho_1,\zeta)\in BC$ and all $(\rho_2,\theta)\in H_2(\rho_{*2},\bar{\theta},K_2)$.
- E3 $\mathscr{Q}_2(Y,\hat{G},\mu,\bar{h})+\mu^\sharp\cos(\bar{\zeta})\sin(\theta)>\bar{\Delta}_2$ for all $(\rho_2,\theta)\in A'F'$ and all $(\rho_1,\zeta)\in H_1(\rho_{*1},\bar{\zeta},K_1)$. Also, $\mathscr{Q}_2(Y,\hat{G},\mu,\bar{h})+\mu^\sharp\cos(\bar{\zeta})\sin(\theta)<-\bar{\Delta}_2$ for all $(\rho_2,\theta)\in C'D'$ and all $(\rho_1,\zeta)\in H_1(\rho_{*1},\bar{\zeta},K_1)$.
- E4 $\mathscr{Q}_2(Y,\hat{G},\mu,\bar{h})>\bar{\Delta}_2$ for all $(\rho_2,\theta)\in F'E'$ and all $(\rho_1,\zeta)\in H_1(\rho_{*1},\bar{\zeta},K_1)$. Also, $\mathscr{Q}_2(Y,\hat{G},\mu,\bar{h})<-\bar{\Delta}_2$ for all $(\rho_2,\theta)\in B'C'$ and all $(\rho_1,\zeta)\in H_1(\rho_{*1},\bar{\zeta},K_1)$.

hold for all values $\hat{G}\in(g_{\min},g_{\max})$ of the parameter estimate for the unknown control gain G. □

Proof: The proof has the same structure as the proof of [14, Lemma 4], except instead of reducing the ρ_{*i}'s and increasing the K_i's to make E1-E4 hold as was done in [14], we choose μ and the $\bar{h}_i$'s big enough. However, the changes needed in the proofs from [14] are significant, so we provide a complete proof here. We assume that

$$\mu>\tfrac{g_{\max}}{g_{\min}}\max\left\{\tfrac{\bar{\zeta}}{\rho_{c1}-\rho_{*1}},\bar{\zeta},\tfrac{\bar{\theta}}{\cos(\bar{\zeta})},\tfrac{\bar{\theta}}{\cos(\bar{\zeta})(\rho_{c2}-\rho_{*2})}\right\}. \tag{17}$$

Later we put more restrictions on μ. We first place conditions on $\bar{h}_1\geq 1$ such that E1 holds for all μ's that satisfy (17).

Since (17) gives $\mu^\sharp=\mu g_{\min}/g_{\max}>\bar{\zeta}/(\rho_{c1}-\rho_{*1})$, we have $\rho_1\leq\rho_{*1}+\bar{\zeta}/\mu^\sharp<\rho_{c1}$ on the leg AB. Also, $\zeta\geq 0$ on AB, the h_i''s are nondecreasing, and $h_1''(\rho_{c1})>0$. Therefore, at all points $Y=(\rho_1,\zeta,\rho_2,\theta)\in H_1(\rho_{*1},\bar{\zeta},K_1)\times H_2(\rho_{*2},\bar{\theta},K_2)$ such that $(\rho_1,\zeta)\in AB$ and for all values $\hat{G}\in[g_{\min},g_{\max}]$, we have $h_1'(\rho_1)\leq h_1'(\rho_{*1}+\bar{\zeta}/\mu^\sharp)<0$, and so

$$\begin{aligned}&\mathscr{Q}_1(Y,\hat{G},\mu,\bar{h})+\mu^\sharp\sin(\zeta)\cos(\theta)\\ &=-\tfrac{\cos(\zeta)\kappa_n}{1-\kappa_n\rho_1-\kappa_g\rho_2}\tfrac{1}{\cos(\theta)}\left(\tfrac{G}{\hat{G}}-\cos^2(\theta)\right)-\tfrac{\alpha\kappa_g\sin(\theta)\sin(\zeta)}{\cos(\theta)}\\ &+\tfrac{Gh_1'(\rho_1)\cos(\zeta)}{\hat{G}\cos(\theta)}-\left\{\tfrac{\sin(\zeta)\mu}{\cos(\theta)}\left(\tfrac{G}{\hat{G}}-\cos^2(\theta)\tfrac{g_{\min}}{g_{\max}}\right)\right\}\\ &\leq\tfrac{1}{\cos(\theta)}\left[||\kappa_n||_\infty\left(\tfrac{g_{\max}}{g_{\min}}+1\right)+||\kappa_g||_\infty\right.\\ &\left.+\tfrac{g_{\min}\cos(\bar{\zeta})h_1'(\rho_{*1}+\bar{\zeta}/\mu^\sharp)}{g_{\max}}\right]<-\bar{\Delta}_1,\end{aligned} \tag{18}$$

when $\bar{h}_1\geq 1$ is large enough, using the nonnegativity of the term in curly braces in (18) along AB, the nonpositivity of the curvatures (which implies that $|\alpha|=|\varphi|/(1-\kappa_n\rho_1-\kappa_g\rho_2)\leq 1$) and the fact that $0<\cos(\bar{\zeta})\leq\cos(\zeta)\leq 1$ on $H_1(\rho_{*1},\bar{\zeta},K_1)\times H_2(\rho_{*2},\bar{\theta},K_2)$, to use $h_1'(\rho_{*1}+\bar{\zeta}/\mu^\sharp)<0$ to cancel the effects of the other terms in (18). The proof that

$$\mathscr{Q}_1(Y,\hat{G},\mu,\bar{h})+\mu^\sharp\sin(\zeta)\cos(\theta)>\bar{\Delta}_1 \tag{19}$$

at all points $(\rho_1,\zeta)\in DE$ for large enough $\bar{h}_1\geq 1$ is analogous, because for all such points, we can use our assumption that $K_1\geq\rho_{c1}$ to get $h_1'(\rho_1)\geq h_1'(\rho_{*1}+\bar{\zeta}/\mu^\sharp+K_1)>0$, and the fact that $\zeta\leq 0$ on the leg DE and nonpositivity of the term in curly braces in (18). This provides our conditions on $\bar{h}_1$ to satisfy E1, which hold for all μ's that satisfy (17).

Next, we specify $\bar{h}_2$'s such that E3 holds for all $\mu\geq 1$ that satisfy (17). Along $A'F'$, condition (17) and our choice of the vertex F′ give $\rho_2\leq\rho_{*2}+\bar{\theta}/[\mu^\sharp\cos(\bar{\zeta})]<\rho_{c2}$, so

$$h_2'(\rho_2)\leq h_2'(\rho_{*2}+\bar{\theta}/[\mu^\sharp\cos(\bar{\zeta})])<0 \tag{20}$$

(because our formulas (4) for the h_i's imply that h_2' is nondecreasing, $h_2'(\rho_{c2})=0$, and $h_2''(\rho_{c2})>0$). Also, $-\pi/2<$

$\theta \le 0$ and so $\sin(\theta) \le 0$ for all pairs (ρ_2, θ) on $A'F'$. Hence,

$$\begin{aligned}
&\mathscr{Q}_2(Y, \hat{G}, \mu, \bar{h}) + \mu^\sharp \cos(\bar{\zeta}) \sin(\theta) \\
&= -\tfrac{\kappa_g \cos^2(\zeta)\cos(\theta)}{1-\kappa_n\rho_1-\kappa_g\rho_2} + \tfrac{G}{\hat{G}}\left(-h_1'(\rho_1)\right. \\
&\left. + \tfrac{\kappa_n}{1-\kappa_n\rho_1-\kappa_g\rho_2}\right)\sin(\zeta)\sin(\theta) \\
&+ \tfrac{G}{\hat{G}}\left(-h_2'(\rho_2) + \tfrac{\kappa_g}{1-\kappa_n\rho_1-\kappa_g\rho_2}\right)\cos(\theta) \\
&+ \left\{\mu \sin(\theta)\left(-\tfrac{G}{\hat{G}}\cos(\zeta) + \tfrac{g_{\min}}{g_{\max}}\cos(\bar{\zeta})\right)\right\} \\
&\ge -||\kappa_g||_\infty + \tfrac{g_{\min}}{g_{\max}}\left|h_2'\left(\rho_{*2} + \tfrac{\bar{\theta}}{\mu^\sharp \cos(\bar{\zeta})}\right)\right|\cos(\bar{\theta}) \\
&- \tfrac{g_{\max}}{g_{\min}}\left(\sin(\bar{\theta})||h_1'||_{[\rho_{*1}, \rho_{*1}+K_1+2]}\right. \\
&\left. + \sin(\bar{\theta})||\kappa_n||_\infty + ||\kappa_g||_\infty\right) \;>\; \bar{\Delta}_2
\end{aligned} \tag{21}$$

at all points $Y \in H_1(\rho_{*1}, \bar{\zeta}, K_1) \times H_2(\rho_{*2}, \bar{\theta}, K_2)$ such that (ρ_2, θ) is on the leg $A'F'$, when $\bar{h}_2 \ge 1$ is large enough (where the lower bound on allowable $\bar{h}_2$'s depends on the choice of $\bar{h}_1$, but not on the choice of μ that satisfies (17)), since the term in curly braces in (21) is nonnegative at such points. To get the inequality in (21), we also used the fact that $\mu^\sharp > \bar{\zeta}$, which follows from (17) and implies that $\rho_{*1} \le \rho_1 \le \rho_{*1} + K_1 + 2$ for all $(\rho_1, \zeta) \in H_1(\rho_{*1}, \bar{\zeta}, K_1)$. Analogous reasoning gives the other assertion in E3, because the term in curly braces in (21) is nonpositive on $C'D'$. Finally, enlarging $\mu \ge 1$ gives conditions E2 and E4. ■

The proof that Theorem 2 leads to our desired robust forward invariance result for the paired hexagons can now be done using the following analog of the proof of [14, Theorem 3] that we gave in [14]. We introduce the constants

$$\begin{aligned}
&\Delta_a^* = \min_{\hat{G}}\{|\mathscr{Q}_1(Y, \hat{G}, \mu, \bar{h}) + \mu^\sharp \sin(\zeta)\cos(\theta)| : \\
&(\rho_1, \zeta) \in AB \cup ED, (\rho_2, \theta) \in H_2(\rho_{*2}, \bar{\theta}, K_2)\}, \\
&\Delta_b^* = \min_{\hat{G}}\{|\mathscr{Q}_1(Y, \hat{G}, \mu, \bar{h})| : (\rho_1, \zeta) \in FE \cup BC, \\
&(\rho_2, \theta) \in H_2(\rho_{*2}, \bar{\theta}, K_2)\}, \\
&\Delta_c^* = \min_{\hat{G}}\{|\mathscr{Q}_2(Y, \hat{G}, \mu, \bar{h}) + \mu^\sharp \cos(\bar{\zeta})\sin(\theta)| : \\
&(\rho_2, \theta) \in C'D' \cup A'F', (\rho_1, \zeta) \in H_1(\rho_{*1}, \bar{\zeta}, K_1)\}, \text{ and} \\
&\Delta_d^* = \min_{\hat{G}}\{|\mathscr{Q}_2(Y, \hat{G}, \mu, \bar{h})| : (\rho_2, \theta) \in B'C' \cup F'E', \\
&(\rho_1, \zeta) \in H_1(\rho_{*1}, \bar{\zeta}, K_1)\},
\end{aligned} \tag{22}$$

where the subscript $\hat{G}$ means that the minimization is also over all constants $\hat{G} \in [g_{\min}, g_{\max}]$. Then $\min\{\Delta_a^*, \Delta_b^*\} \ge \bar{\Delta}_1$ and $\min\{\Delta_c^*, \Delta_d^*\} \ge \bar{\Delta}_2$, where $\bar{\Delta}_i$ is the known bound on $|\delta_i(t)|$ for $i = 1, 2$ as before, and our results apply for any choices $\bar{\Delta}_i \ge 0$. Set $\bar{\Delta}_\zeta = \min\{\Delta_a^*, \Delta_b^*\}$ and $\bar{\Delta}_\theta = \min\{\Delta_c^*, \Delta_d^*\}$. The following implies that our adaptive tracking and parameter identification dynamics (5) has the robustly forwardly invariant set $H_1(\rho_{*1}, \bar{\zeta}, K_1) \times H_2(\rho_{*2}, \bar{\theta}, K_2) \times (g_{\min}, g_{\max})$ for suitable perturbation sets $\mathscr{D}$:

Corollary 1: Let $(\bar{\zeta}, \bar{\theta}) \in (0, \pi/2)^2$, $(\bar{\Delta}_1, \bar{\Delta}_2) \in [0, \infty)^2$, and $(\rho_{*1}, \rho_{*2}, K_1, K_2) \in (0, \rho_{c1}) \times (0, \rho_{c2}) \times [\rho_{c1}, \infty) \times [\rho_{c2}, \infty)$ be given constants, and choose any constant vector $(\mu, \bar{h}_1, \bar{h}_2)$ such that conditions E1-E4 from Lemma 2 hold. Then: (a) For each C^1 solution $\hat{G} : [0, \infty) \to (g_{\min}, g_{\max})$ of the update law (12) and all constants $\delta_{*1} \in (0, \bar{\Delta}_\zeta)$ and $\delta_{*2} \in (0, \bar{\Delta}_\theta)$, the set $\mathscr{H} = H_1(\rho_{*1}, \bar{\zeta}, K_1) \times H_2(\rho_{*2}, \bar{\theta}, K_2)$ is robustly forwardly invariant for (13) with the disturbance set $\mathscr{D} = [-\delta_{*1}, \delta_{*1}] \times [-\delta_{*2}, \delta_{*2}]$. (b) For each constant $\delta_+ > \bar{\Delta}_\zeta$ (resp., $> \bar{\Delta}_\theta$), there exist a boundary point $Y \in \partial(H_1(\rho_{*1}, \bar{\zeta}, K_1) \times H_2(\rho_{*2}, \bar{\theta}, K_2))$ and a solution of (12) such that the trajectory for (13) starting at Y for one of the constant perturbations $\pm(\delta_+, 0)$ (resp., $\pm(0, \delta_+)$) exits $H_1(\rho_{*1}, \bar{\zeta}, K_1) \times H_2(\rho_{*2}, \bar{\theta}, K_2)$ in finite time. □

Proof: The proof of Corollary 1 has the same structure as the proof of [14, Theorem 3], with the important difference that instead of using conditions (C1)-(C4) from [14, Lemma 4], we use the corresponding conditions E1 and E3 (resp., E2 and E4) to prevent trajectories from exiting through the tilted (resp., top and bottom) legs of the paired hexagons. ■

By combining Theorem 1 and Corollary 1, we can prove that for all constants $\bar{\Delta}_i \ge 0$ for $i = 1, 2$ and each choice of $\mathscr{D}$ that satisfies the requirements from Corollary 1, the system (5) is input-to-state stable with respect to its equilibrium $(\rho_{c1}, 0, \rho_{c2}, 0, G)$ on each set $H_1(\rho_{*1}, \bar{\zeta}, K_1) \times H_2(\rho_{*2}, \bar{\theta}, K_2) \times (g_{\min}, g_{\max})$ with perturbations $\delta = (\delta_1, \delta_2)$ that are valued in $\mathscr{D}$. This follows from the boundedness of the gradient of U on any of the compact paired hexagons, and [14, Lemma 2]. This implies curve tracking and identification of the control gain G, in the special case where the perturbations δ_i are 0. We next compare the preceding algorithm with the algorithm from [14] in detail.

IV. Comparing Algorithms

Section III provides a very different way to find tolerance and safety bounds from the method in [14, Remark 2]. To see why, we first express the method from [14, Remark 2] as follows, where the legs refer to those of $H_1(\rho_{*1}, \bar{\zeta}, K_1) \times H_2(\rho_{*2}, \bar{\theta}, K_2)$ from Fig. 1 above, as before:

Algorithm 1: Given any positive constants $\bar{\Delta}_i$ such that the unknown perturbation δ_i in (5) is known to take all of its values in $[-\bar{\Delta}_i, \bar{\Delta}_i]$ for $i = 1$ and 2, any pairs $(\rho_{c1}, \rho_{c2}) \in (0, \infty)^2$ and $(\bar{\zeta}, \bar{\theta}) \in (0, \pi/2)^2$, and any common value $c = \bar{h}_1 = \bar{h}_2 > 0$ for the constants in the formula (4) for the penalty functions h_i, choose the constants $\mu > 0$ and $\rho_{*i} \in (0, \rho_{ci})$ and $K_i > 0$ for $i = 1$ and 2 using the following steps:

- S1 Choose $\mu > 0$ and constants $\bar{\rho}_{*i} \in (0, \rho_{ci})$ for $i = 1, 2$ such that (17) holds for all $\rho_{*i} \in (0, \bar{\rho}_{*i})$ for $i = 1, 2$.
- S2 Choose $\rho_{*1} \in (0, \bar{\rho}_{*1})$ small enough and $K_1 \ge \rho_{c1}$ large enough such that for all μ satisfying S1, we have:
  - G1 $\mathscr{Q}_1(Y, \hat{G}, \mu, \bar{h}) + \mu^\sharp \sin(\zeta)\cos(\theta) < -\bar{\Delta}_1$ (resp., $> \bar{\Delta}_1$) at all points on the leg AB (resp., DE).
- S3 Choose $\rho_{*2} \in (0, \bar{\rho}_{*2})$ small enough and $K_2 \ge \rho_{c2}$ large enough such that for all μ satisfying S1, we have:
  - G2 $\mathscr{Q}_2(Y, \hat{G}, \mu, \bar{h}) + \mu^\sharp \cos(\bar{\zeta})\sin(\theta) > \bar{\Delta}_2$ (resp., $< -\bar{\Delta}_2$) at all points on the leg A′F′ (resp., C′D′).
- S4 Enlarge $\mu > 0$ as needed to satisfy E2 and E4.

Then $H_1(\rho_{*1}, \bar{\zeta}, K_1) \times H_2(\rho_{*2}, \bar{\theta}, K_2) \times (g_{\min}, g_{\max})$ is robustly forwardly invariant for the augmented system (5) for all disturbances δ valued in $\mathscr{D} = [-\bar{\Delta}_1, \bar{\Delta}_1] \times [-\bar{\Delta}_2, \bar{\Delta}_2]$. □

While not explicitly stated in [14], Algorithm 1 follows from the proof of [14, Lemma 4] and uses the properties $\lim_{\rho_i \to 0^+} h_i(\rho_i) = \lim_{\rho_i \to \infty} h_i(\rho_i) = \infty$ for $i = 1, 2$ to pick the ρ_{*i}'s small enough and the K_i's big enough. The choices of ρ_{*2} and K_2 in Step S3 depend on the choices of ρ_{*1} and K_1 from Step S2. If we use Algorithm 1, then larger perturbation

bounds $\bar{\Delta}_i$ require choosing smaller positive constants ρ_{*i} and larger K_i's, so the hexagons get close to the vertical axes in Fig. 1, and also become wider (which corresponds to allowing the robot to move far from the curve being tracked).

By contrast, our new algorithm from Section III is as follows, where conditions G1-G2 are from Algorithm 1:

Algorithm 2: Given any positive constants $\bar{\Delta}_i$ such that the unknown perturbation δ_i in (5) is known to take all of its values in $[-\bar{\Delta}_i, \bar{\Delta}_i]$ for $i = 1$ and 2, any pairs $(\rho_{c1}, \rho_{c2}) \in (0,\infty)^2$ and $(\bar{\zeta}, \bar{\theta}) \in (0, \pi/2)^2$, and any constants $\rho_{*i} \in (0, \rho_{ci})$ and $K_i \geq \rho_{ci}$ for $i = 1$ and 2, choose the constant $\mu > 0$ and the scaling constants $\bar{h}_i$'s in (4) as follows:

M1 Choose any constant $\mu > 0$ such that (17) holds.
M2 Choose $\bar{h}_1$ such that G1 holds for all μ satisfying (17).
M3 Choose $\bar{h}_2$ such that G2 holds for all μ satisfying (17).
M4 Enlarge $\mu > 0$ as needed to satisfy E2 and E4.

Then $H_1(\rho_{*1}, \bar{\zeta}, K_1) \times H_2(\rho_{*2}, \bar{\theta}, K_2) \times (g_{\min}, g_{\max})$ is robustly forwardly invariant for the augmented system (5) for all disturbances δ valued in $\mathscr{D} = [-\bar{\Delta}_1, \bar{\Delta}_1] \times [-\bar{\Delta}_2, \bar{\Delta}_2]$. □

Since $\mathscr{Q}_2(Y, \hat{G}, \mu, \bar{h}) + \mu^\sharp \cos(\bar{\zeta}) \sin(\theta)$ depends on h_1, the $\bar{h}_2$ in Step M3 will depend on $\bar{h}_1$. Algorithm 2 scales the h_i's by increasing the $\bar{h}_i$'s, instead of using the approach from Algorithm 1 of manipulating the arguments of the h_i's. Algorithm 2 eliminates the need to allow the paired hexagons to get too wide or close to the vertical axes in Fig. 1, which is helpful in applications that require separation between the robot and the curve being tracked; see (16). By proving ISS under arbitrarily large $\bar{\Delta}_i$'s, under scalings of μ and of the $\bar{h}_i$'s, while maintaining positive distances between the paired hexagons and the edges of the state space, our work also improves on the ISS results from [14], which did not use our scaling approach and did not compensate for arbitrarily large disturbances unless the distances from the paired hexagons to the edges of the state space decreased towards zero.

V. Conclusions

We advanced the theory of state constrained 3D curve tracking by exploiting connections between tuning constants and allowable perturbation bounds that ensure robust forward invariance. Our new results include perturbations, polygonal state constraints, and identification of unknown control gains using adaptive control. Our scaling approach tunes scaling constants in the controls to compensate for arbitrarily large disturbance bounds while maintaining desirable separation between the polygons and the edges of the state space, and so builds on [14, Remark 2] from our recent *SIAM Journal on Control and Optimization* paper. We hope to extend our work to identify the curvatures κ_n and κ_g when the curvatures are unknown, which is challenging because the curvatures enter (5) in a nonlinear way. This would generalize our scaling method from [10] for identifying unknown curvatures in the 2D case, which used one scaling parameter instead of the three scaling constants μ, $\bar{h}_1$, and $\bar{h}_2$ that we needed here.

References

[1] A. Aguiar and J. Hespanha. Trajectory-tracking and path-following of underactuated autonomous vehicles with parametric modeling uncertainty. *IEEE Transactions on Automatic Control*, 52(8):1362-1379, 2007.

[2] E. Justh and P. Krishnaprasad. Natural frames and interacting particles in three dimensions. In *Proceedings of the 44th IEEE Conference on Decision and Control and European Control Conference (Seville, Spain, 12-15 December 2005)*, pp. 2841-2846.

[3] H. Khalil. *Nonlinear Systems, Third Edition*. Prentice-Hall, Upper Saddle River, NJ, 2002.

[4] M. Krstic, I. Kanellakopoulos, and P. Kokotovic. *Nonlinear and Adaptive Control Design*. John Wiley and Sons, New York, 1995.

[5] M. Krstic and A. Smyshlyaev. Adaptive control of PDEs. *Annual Reviews in Control*, 32:149-160, 2008.

[6] E. Lefeber, K. Pettersen, and H. Nijmeijer. Tracking control of an underactuated ship. *IEEE Transactions on Control Systems Technology*, 11(1):52-61, 2003.

[7] R. Lenain, B. Thuilot, C. Cariou, and P. Martinet. High accuracy path tracking for vehicles in presence of sliding: Application to farm vehicle automatic guidance for agricultural tasks. *Autonomous Robots*, 21(1):79-97, 2006.

[8] M. Malisoff and F. Mazenc. *Constructions of Strict Lyapunov Functions*. Communications and Control Engineering Series, Springer-Verlag London Ltd., London, UK, 2009.

[9] M. Malisoff, F. Mazenc, and F. Zhang. Stability and robustness analysis for curve tracking control using input-to-state stability. *IEEE Transactions on Automatic Control*, 57(5):1320-1326, 2012.

[10] M. Malisoff, R. Sizemore, and F. Zhang. Adaptive planar curve tracking control and robustness analysis under state constraints and unknown curvature. *Automatica*, to appear.

[11] M. Malisoff and F. Zhang. Adaptive control for planar curve tracking under controller uncertainty. *Automatica*, 49(5):1411-1418, 2013.

[12] M. Malisoff and F. Zhang. Robustness of a class of three-dimensional curve tracking control laws under time delays and polygonal state constraints. In *Proceedings of the American Control Conference (Washington, DC, 17-19 June 2013)*, pp. 5710-5715.

[13] M. Malisoff and F. Zhang. An adaptive control design for 3D curve tracking based on robust forward invariance. In *Proceedings of the 52nd IEEE Conference on Decision and Control (Florence, Italy, 10-13 December 2013)*, pp. 4473-4478.

[14] M. Malisoff and F. Zhang. Robustness of adaptive control under time delays for three-dimensional curve tracking. *SIAM Journal on Control and Optimization*, 53(4):2203-2236, 2015.

[15] F. Mazenc and M. Malisoff. Strict Lyapunov function constructions under LaSalle conditions with an application to Lotka-Volterra systems. *IEEE Transactions on Automatic Control*, 55(4):841-854, 2010.

[16] S. Mukhopadhyay, C. Wang, M. Patterson, M. Malisoff, and F. Zhang. Collaborative autonomous surveys in marine environments affected by oil spills. In *Cooperative Robots and Sensor Networks 2014*. Studies in Computational Intelligence Series Vol. 554, Springer, New York, 2014, pp. 87-113.

[17] C. Samson. Control of chained systems: Application to path-following and time-varying point-stabilization of mobile robots. *IEEE Transactions on Automatic Control*, 40(1):64-77, 1995.

[18] C. Woolsey and L. Techy. Cross-track control of a slender, underactuated AUV using potential shaping. *Ocean Engineering*, 36(1):82-91, 2009.

[19] X. Xiang, L. Lapierre, C. Liu, and B. Jouvencel. Path tracking: combined path following and trajectory tracking for autonomous underwater vehicles. In *Proceedings of the IEEE/RSJ International Conference on Intelligent Robots and Systems (San Francisco, CA, 25-30 September 2011)*, pp. 3558-3563.

[20] F. Zhang, D. Fratantoni, D. Paley, J. Lund, and N. Leonard. Control of coordinated patterns for ocean sampling. *International Journal of Control*, 80(7):1186-1199, 2007.

[21] F. Zhang, E. Justh, and P. Krishnaprasad. Boundary following using gyroscopic control. In *Proceedings of the 43rd IEEE Conference on Decision and Control (Paradise Island, Bahamas, 14-17 December 2004)*, pp. 5204-5209.

[22] F. Zhang, E. Justh, and P. Krishnaprasad. Boundary tracking and obstacle avoidance using gyroscopic control. In *Recent Trends in Dynamical Systems: Proceedings of a Conference in Honor of Jürgen Scheurle*. Springer, Basel, Switzerland, 2013, pp. 417-446.

[23] F. Zhang, A. O'Connor, D. Luebke, and P. Krishnaprasad. Experimental study of curvature-based control laws for obstacle avoidance. In *Proceedings of the IEEE International Conference on Robotics and Automation (New Orleans, LA, 26 April-1 May 2004)*, pp. 3849-3854.